

INSTRUMENTATION AND TECHNOLOGY SUPPORTING THE EVENT HORIZON TELESCOPE

Jonathan Weintroub on behalf of the Event Horizon Telescope Collaboration¹

RESUMEN

El Event Horizon Telescope (EHT) es un arreglo interferométrico de línea de base muy larga (VLBI, por sus siglas en inglés) del tamaño de la Tierra, que opera en las longitudes de onda de radio más cortas, de aproximadamente 1 milímetro, correspondientes a frecuencias de radio de 230 GHz y superiores. Como resultado, tiene una resolución angular extremadamente fina, del orden de 20 microarcosegundos. Para los agujeros negros supermasivos (SMBH, por sus siglas en inglés) relativamente cercanos y suficientemente masivos, ésta es la escala angular subtendida por el horizonte de eventos. La emisión relativista con efecto *lensing* del disco de acreción y del *jet* del agujero negro puede observarse directamente. La primera imagen de la “sombra” del horizonte de eventos del agujero negro de M87 y SgrA*, en el centro de la Vía Láctea, se obtuvo gracias a la adaptación de la nueva tecnología de banda ancha y los relojes atómicos a los radiotelescopios existentes. En una charla en un simposio para celebrar el 60avo aniversario del Instituto Argentino de Radioastronomía, di una introducción a la ciencia detrás del EHT, mostré la imagen de intensidad de M87 publicada en 2019, imágenes de polarización publicadas en 2021, y la imagen del SMBH del Centro Galáctico publicada en 2022, el año del simposio. Con las imágenes como motivación, el enfoque principal de mi charla fue describir la tecnología y la instrumentación que permitieron las observaciones. Este artículo documenta la citada charla.

ABSTRACT

The Event Horizon Telescope (EHT) is an earth-size very long baseline interferometry (VLBI) array, operating at the shortest radio wavelengths of about 1 millimeter, corresponding to radio frequencies 230 GHz and higher. As a result it has an extremely fine angular resolution of the order of 20 microarcseconds. For super massive black holes (SMBH) which are relatively nearby and sufficiently massive, this is the angular scale subtended by the event horizon. Relativistically lensed emission from the black hole’s accretion disk and jet can be directly observed. Retrofitting new wideband technology and atomic clocks to existing radio telescopes led to the first image of the “shadow” of the event horizon of the black hole in M87 and SgrA* at the center of the Milky Way. In a talk at a symposium celebrating the 60th Anniversary of the Instituto Argentino de Radioastronomía (IAR), I gave an introduction to the science behind the EHT, showed the intensity image of M87 published in 2019, polarization images published in 2021, and the image of the Galactic Center SMBH published in 2022, the year of the symposium. With the images as motivation, the main focus of my talk was to describe the technology and instrumentation which enabled the observations. This short paper documents my symposium talk.

Key Words: Digital Signal Processing — Black Hole Imaging — Instruments — Event Horizon Telescope

1. INTRODUCTION

Several key instrument developments have enabled the extension of the very long baseline interferometry (VLBI) technique to Event Horizon Telescope (EHT) observing wavelengths. To meet sensitivity requirements, high-bandwidth digital systems were developed that process data at rates of 64 gigabits per second (Gbps), exceeding cm-wavelength VLBI arrays by more than an order of magnitude. Associated improvements include the development of phasing systems at array facilities, new receiver

installation at several sites, and the deployment of hydrogen maser frequency standards to ensure coherent data capture across the array.

As radio astronomy receiver bandwidth has increased, it has become necessary to increase the speed of analog-to-digital conversion (ADC) or sampling, as well as the digital signal processing (DSP) in the telescope’s back end. The alternative “hybrid” approach requires a complex and expensive mixer-filter system to break the IF bandwidth into smaller blocks for digital sampling and signal processing. ADCs capable of sample rates five gigasamples-per-second (GSa/s) and faster are now available (see

¹Center for Astrophysics | Harvard & Smithsonian, Cambridge, MA, USA; www.eventhorizontelescope.org

Table 1) and DSP technology has been following Moore's Law to provide matching processing power. In current EHT wideband instruments, usable bandwidth blocks ~ 2 GHz can be processed digitally. In future EHT deployments blocks ~ 8 GHz are pre-processed and sampled by a single compact module. Ultra-wideband ADC and DSP technology and wideband processing in radio astronomy digital back ends, recorders, correlators and phased arrays have been essential to the instrumentation which supports the Event Horizon Telescope.

This paper, which documents the talk given at the IAR 60th Anniversary symposium, will show and briefly discuss the EHT's legacy of event-horizon-scale images of M87 and SgrA* published between 2019 and 2022. Then it describes a selection of instrument developments which enabled the observation. All of the images and instruments described in this paper have been previously published, most of them by the EHT Collaboration (EHTC).

2. A BRIEF LOOK AT THE EHT IMAGES

The premise of the EHT is the extension of VLBI observations to shorter wavelengths ~ 1.3 mm. The EHT targets supermassive black holes with the largest apparent event horizons: M87 in Virgo and Sgr A* in the Galactic Center. The compact size of SgrA* was confirmed in 2007 by studies at 1.3 mm, using baselines that ran from Hawai'i to the mainland US.

During 5-11 April 2017, the EHT observed M87 and calibrators on four separate days using an array that included eight radio telescopes at six geographic locations: Arizona (USA), Chile, Hawai'i (USA), Mexico, the South Pole, and Spain; see Fig. 1: image from The Event Horizon Telescope Collaboration et al. (2019a). In 2021 the same 2017 data was processed to yield the polarization image shown in Fig. 2, image from The Event Horizon Telescope Collaboration et al. (2021).

And in 2022 the EHT published the first image of the 4 million solar mass black hole in SgrA* (see Fig. 3). The ring and shadow on similar angular scales to M87 are seen in this much less massive SMBH, while three bright regions are seen in the ring, as opposed to one bright region in the South for M87 which is ~ 6 billion solar masses (The Event Horizon Telescope Collaboration et al. 2022).

3. EHT INSTRUMENTATION

The remainder of this paper will describe some of the instrumentation which was developed to make these images possible. A detailed description of the

system design of the instrument is in The Event Horizon Telescope Collaboration et al. (2019b).

3.1. How VLBI works

There is a general principle that the diffraction limited resolution of a lens is inversely proportional to its diameter, where the diameter is measured in units of a wavelength. VLBI places telescopes across the globe to form an earth-size virtual telescope. VLBI has been done for decades, but the EHT has stretched the techniques to the shortest possible radio wavelengths, thereby providing the finest angular resolutions available from any terrestrial VLBI array. A single baseline samples a single spatial frequency, and longer baselines, measured in units of wavelengths, sample higher frequencies. Figure 4 shows schematically the principal of VLBI and the components of the system.

Separating the telescopes by this distance means technical and logistical challenges. These include the need for atomic clocks because it is not practical to distribute a common reference to each telescope. It also results in the need to record on disk drives and fly them to a central location for processing. The earth rotates and this is key to the sampling of different spatial frequencies of the image, but also means the system needs to track the changing delay and changing Doppler shift from station to station. Figure 5 shows the extreme precision of the atomic clock measured in terms of Allan Deviation, against a crystal standard, and long term drift against GPS time.

3.2. Wideband samplers

In a sampled data system the width of a single block of processed bandwidth is set by the ADC sample rate through the Nyquist criterion. If the block is narrow, the processor must be preceded by an IF system with many channels; a so called "hybrid" implementation, which, if large, is likely to be cost-prohibitive. While digital technology becomes exponentially more economical with time per unit processing power, according to Moore's law, this law does not apply to analog IF electronics, which typically increases in cost over time. Thus costs of large systems—where the non-recurring cost of high performance design is amortized over many units—are reduced if they are designed with using ADCs which are as fast as possible.

It is necessary that the fast ADC chip must be matched to DSP technologies with commensurate input-output data bandwidth, and processing power. A useful technology is the Field Programmable Gate Array (FPGA). FPGAs are now equipped with asynchronous serializer-deserializer input-output devices

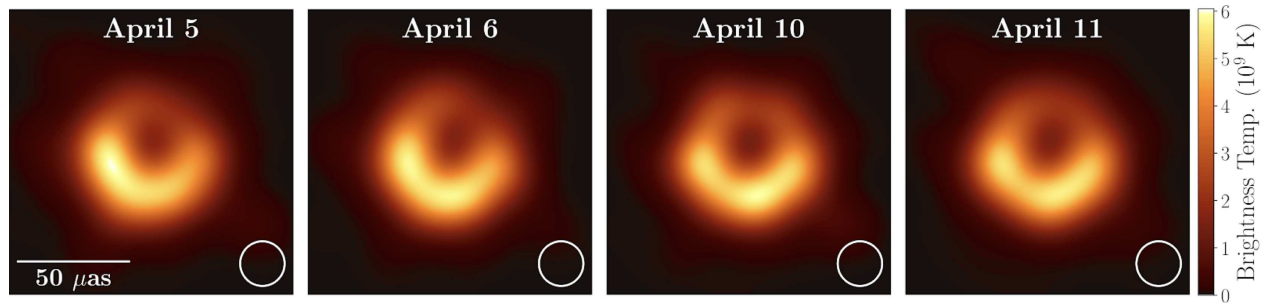


Fig. 1. The EHT made images of M87 on four days in 2017 two pairs of which were successive. These were published in April 2019. Similar images taken over different days show the stability of the basic image structure and effectively repeat the experiment on different days, with the consistency of the independent images contributing to confidence in the image.

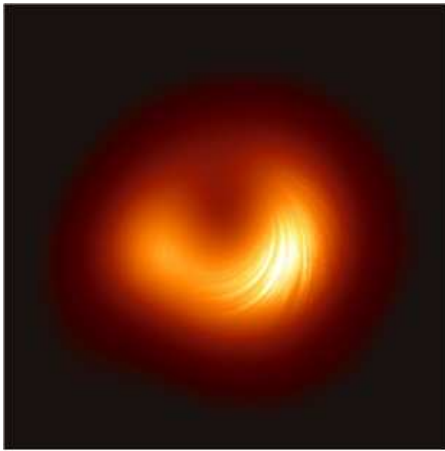


Fig. 2. In 2021 images showing the polarization structure within the ring were published, also using the data from 2017. Polarization vectors allow tracing the magnetic fields in the accretion disk. For details on reduction and interpretation, see The Event Horizon Telescope Collaboration et al. (2021).

(SERDES). For the GTY series of SERDES included on the Xilinx Ultrascale+ family input-output data rates in excess of 30 Gbps is possible. An essential function of the SERDES is to demultiplex the very high bitrate from the fast ADC chip, so that the FPGA, with typical maximum fabric speeds of around 500 MHz, can process the data stream in real time over many parallel logic paths. The availability of this fast SERDES silicon intellectual property is one key factor giving the FPGA an edge over Application Specific Integrated Circuits (ASICs) when considered for fast DSP applications—even in relatively high volume radio astronomy applications. Another key benefit is the provision of large numbers of wide fixed point multipliers, with as many as

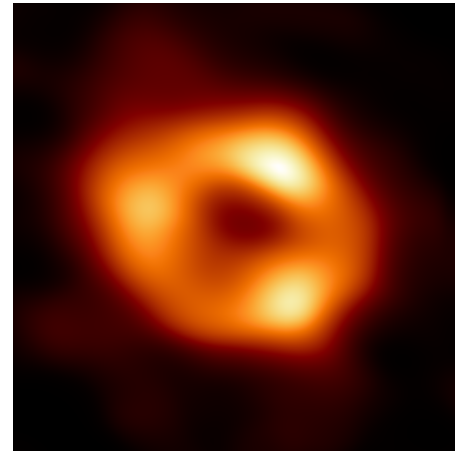


Fig. 3. In 2022 the first image of the black hole at the center of the Milky Way was published. The ring and shadow are again visible for this very much less massive black hole ~ 4 million solar masses. The angular size is actually slightly larger than for M87 because SgrA* is 26,000 light years distant as opposed to 55 million light years for M87. SgrA* has a much shorter time scale of variability making it more challenging to image than M87.

12,288 DSP slices each equipped with one multiplier in the Xilinx Ultrascale+ VU13P DSP optimized device.

Many ADCs achieve high sample rates by interleaving multiple slower ADC cores. Distortion results from misalignment in offset, gain and phase of the cores, as well as non-linearity. It is possible to align the cores and calibrate non-linearity resulting in substantially improved fidelity. Successful wide-band instruments have been designed using multi-core ADCs. Still, absent other constraints, single core devices are preferred. The faster the sample rate of an ADC the greater the Nyquist bandwidth,

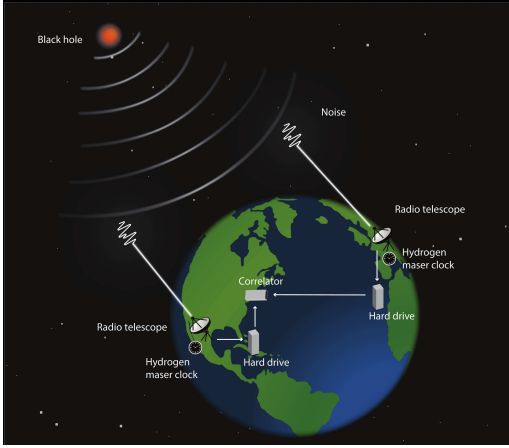


Fig. 4. Showing the principal of VLBI: telescope separated widely across the earth, scheduled to point at the same source during a time of mutual visibility, and each with a hydrogen maser clock and data recorder.

but the ability of an ADC to handle a wideband analog signal is determined by a distinct specification, analog bandwidth. The number of bits of conversion is also key, typically, though, single core fast devices have relatively few bits. We view four bits as effectively the minimum requirements for current instrument development. In case of correlators, four bits delivers 99% digital efficiency.

An important document covering the evaluation of the performance of ADCs is IEEE Standard 1241-2010 - Terminology and Test Methods for Analog-to-Digital Converters². For the noiselike signals common in radio astronomy the Noise Power Ratio (NPR) specification is of particular interest. Table 1 shows a snapshot listing of various ADCs we have considered with sample rates 5 GSa/s and greater, in increasing order of sample frequency (f_s). The EV8AQ160 is used in SMA SWARM and the R2DBE for EHT, and ASNT713A-KMA is under development for ngEHT (ngDBE) and the wSMA D-engine.

3.3. VLBI Beamformers: SWARM

The SMA Wideband Astronomical ROACH2 Machine (SWARM, Primiani et al. 2016) is a 32 GHz bandwidth VLBI capable correlator and VLBI phased array designed and deployed at the Smithsonian Astrophysical Observatory’s Submillimeter Array (SMA) in 2017, see Fig. 6. The SMA is an eight-element radio interferometer located atop Maunakea in Hawai’i. Eight six-meter dishes may be arranged into configurations with baselines as long

²<https://ieeexplore.ieee.org/document/5692956>

TABLE 1: Summary table of high speed ADC devices candidates 5 GSa/s and greater, with relevant specifications and pricing.

f_s (GSa/s)	cores	BW (GHz)	bits	Manufacturer	Part #	~cost	remarks
5	4	2.0	8	e2v	EV8AQ160	\$300	ASIAA/Jiang SWARM
6.4	4	>10	12	TI	ADC12DJ3200	\$2196	COTS in stock
12	1	20	4	Adantec	ASNT7120-KMA	\$800	3.5 ENOB, 2W, ZDOK
12.5		8	8	Tektronix Comp.	—	\$17k	formerly Maxtek
16.384	1	20	4	Adantec	ASNT713A-KMA	\$2.4k	single core; ngEHT & wSMA
20	4/2	8	5	e2v	EV5AS210	\$7k	used for NOEMA, discount.
20		13	8	Keysight	—	—	
20	1	10	3+oflow	Analog Dev.	HMC5401LC5	\$2,863k	was Hittite, SAO eval.
20	4/5		6	Pacific Microchip	SBIR funded	\$3-5k	JESD204B,
25	1	22	4	Alphacore	SBIR funded	—	w/ SERDES, not COTS yet
34	4	20+	6	Micram	ADC3401/2	\$47k	module, ADC30
56	64	20	8	Pacific Microchip	SBIR funded	\$3-5k	
56		13	68	Guzik	WDM5121	—	snapshot, 4 Gpt memory
42 - 68		25	10	Jarjet	Williamson ADC	—	ASIC IP macro only
56	320	15	8	Fujitsu/SoCIONext	Robin/Blackbird	\$20k	CHAIS, Vadatech

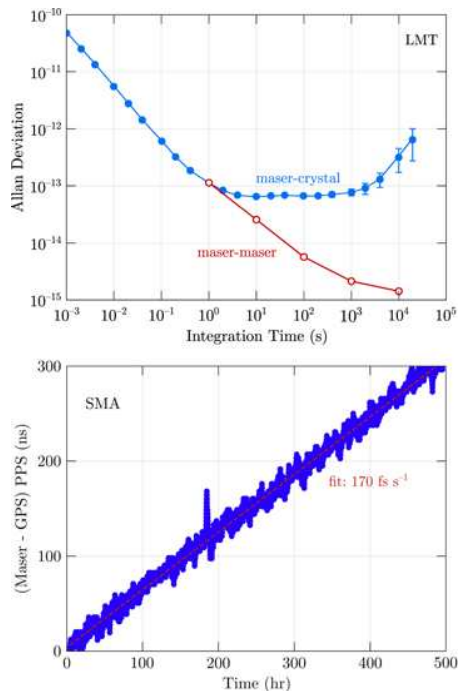


Fig. 5. Hydrogen maser time standards are the atomic clocks needed to maintain coherence at different EHT sites. The top panel shows Allan deviation measured against a fine quartz crystal oscillator (OXCO), using the Large Millimeter Telescope (LMT). The bottom panel shows long term drift against the real time reference distributed by the GPS network, measured at the Submillimeter Array (SMA). This reference is intrinsically better than the maser, if diurnal variations and other instabilities imposed on the GPS real time signal by the earth's atmosphere are averaged out over several days (The Event Horizon Telescope Collaboration et al. 2019b).

as 509 m, producing a synthesized beam of sub-arcsecond width at 345 GHz. SWARM was developed when the SMA expanded the bandwidth of its receiver sets to 12 GHz in each sideband. Dual polarized receivers can be operated simultaneously in a single band. Counting both sidebands and both polarizations, the total bandwidth of the SMA is 48 GHz. This sets the most fundamental and demanding requirement for SWARM, that the instantaneous processed bandwidth match the aggregate bandwidth of the receivers.

The four core 5 GSa/s e2v EV8AQ160³ has been studied in depth (Patel et al. 2014). The device provides register controls to align the cores to reduce the impact of spurs which arise due to misalignment

³<http://www.e2v.com/resources/account/download-datasheet/2291>

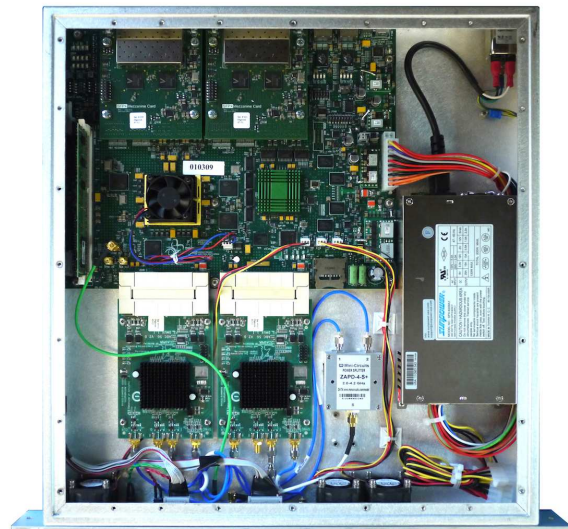


Fig. 6. Plan view photo of the ROACH2 platform configured for SWARM. Two 5 GSa/s Quad Core ADCs are plugged into connectors towards the bottom, providing samples at a data rate approaching 80 Gbps. Eight 10 Gigabit Ethernet ports on the mezzanine board towards the top provide matched data rate throughput to the network switch. Photo credit: Derek Kubo.

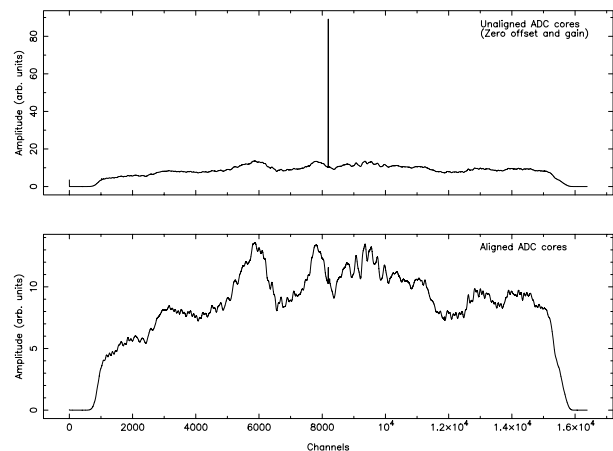


Fig. 7. Autocorrelation spectrum obtained from one of the ADCs, over a 30 second integration. The top panel shows the spectrum with the offset and gain parameters set to zeroes, for the four cores of the ADC. It shows a strong spur near the center, and a weaker spur in the first channel. The bottom panel shows that setting the offset and gain values removes the spurs effectively.

in offset, gain, phase (OGP), or threshold Integral Non-Linearity (INL). All the cores are clocked by the same external clock input. The quad 1.25 GSa/s interleaved mode has an equivalent sampling frequency

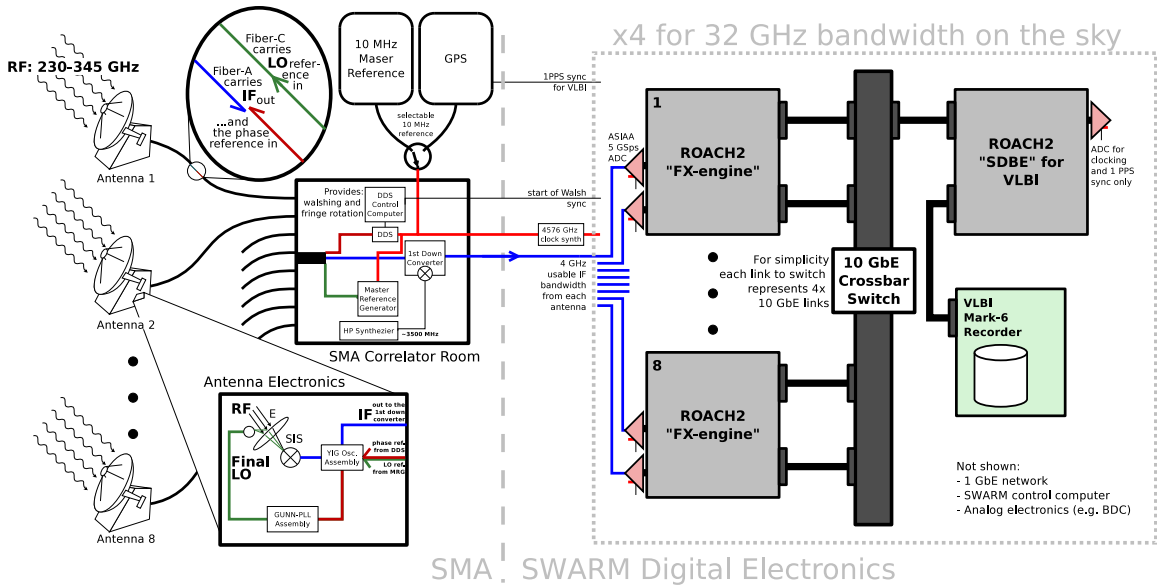


Fig. 8. Block diagram showing at the top level a quadrant of SWARM, on the right of the dotted line, in the context of legacy SMA systems on the left. There are eight ROACH2s on the left of the 10 GbE crossbar switch, which contain F- and X-engines, as well as coarse and fine delay tracking, phase control and deWalshing, a phased array summer, visibility accumulator, network logic, and assorted transposes and other memory. On the right hand side of the switch is shown the SDBE and Mark6 data recorder, both required for EHT VLBI.

of 5 GSa/s. A Collaboration for Astronomy Signal Processing and Electronics Research (CASPER, Hickish et al. 2016) compatible printed circuit board is available based on this ADC, designed by Jiang et al. (2014). Patel et al. (2014) detail how the OGP and INL corrections are derived, and Fig. 7 shows the autocorrelation spectra obtained with one of the ADCs, and the improvement obtained using core alignment.

The SWARM sample rate of 4.576 GHz results in an approximately 2.3 GHz Nyquist bandwidth, with the upper edge of the usable 2 GHz band at 2.15 GHz. While the bandwidth of the e2v ADC in the data sheet is 2.0 GHz, our frequency response measurements show that the device responds beyond that limit, with the attenuation at 2.15 GHz about 6 dB. A sample rate of 4.6 GSa/s is within the maximum specified rate.

CASPER pioneered the use of a commercial Ethernet switch as DSP interconnection fabric (Parsons et al. 2008). Data is packetized prior to transmission via Ethernet switch “crossbar” from F-engine to X-engine and to VLBI recorders. SWARM uses this approach to integrate two instruments: a correlator with 140 kHz spectral resolution across its full 32 GHz band, used for connected interferometric observations, and a phased array mode (Young et al. 2016) used when the SMA becomes a station in the

EHT.

Each SWARM quadrant ROACH2 units (Fig. 6), shared under open source by CASPER, are equipped with a pair of ultra-fast ADCs, a FPGA processor, and eight 10 Gigabit Ethernet (GbE) ports. A VLBI data recorder interface designated the SWARM Digital Back End, or SDBE, is implemented with a ninth ROACH2 per quadrant, feeding four Mark6 VLBI recorders with an aggregate recording rate of 64 Gbps. See Figure 8 which shows the architecture of a single SWARM quadrant at the top level, with the right hand side of the drawing showing the basic CASPER concept of processing engines organized around a 10 GbE switch.

3.4. EHT single dish instrumentation

The developments at the Submillimeter Array demonstrate the feasibility of ultra-wide band digital processing with fine uniform spectral resolution and VLBI capability. Figure 9 is a 32 GHz wide instantaneous contiguous spectrum with 140 kHz uniform spectral resolution, an impressive demonstration of what is possible. A ROACH2 configured identically with dual 5 Gsps ADC boards is used as the primary digital back end at single dish EHT stations. The ROACH2 runs with a different FPGA bitcode or “personality”, and in this mode is called the *R2DBE* (Vertatschitsch et al. 2015); see also Fig. 10.

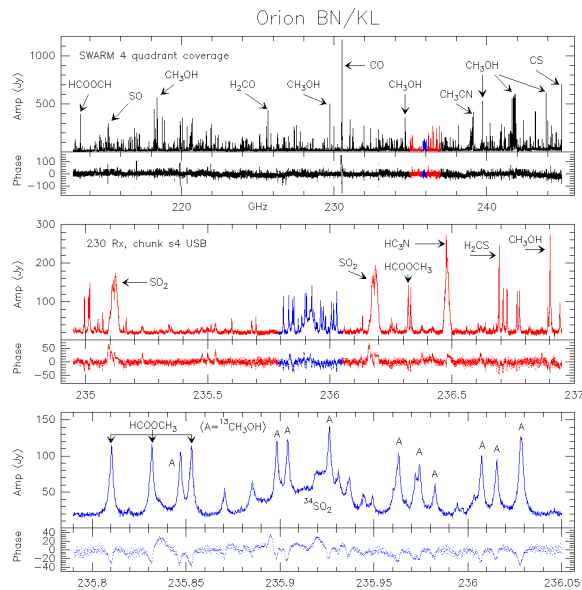


Fig. 9. The spectrum of Orion BN/KL covering an instantaneous 32 GHz on the sky with 140 kHz resolution uniformly available across the full bandwidth. The data were taken on 26 January 2017 UTC with SWARM. From the top, the three panels show: the full 32 GHz, a single 2.0 GHz ‘chunk’ from one of 16 IF-ADC channels, and a detail of just over 200 MHz span, revealing the fine structure available in *all the data*—the 200 MHz blue fragment could be placed anywhere to reveal similar detail.

3.5. The path to future wideband subsystems

An upgrade of the SMA designated *wSMA* envisions a quadrupling of the present 32 GHz SMA bandwidth to 128 GHz. This is achieved by a further doubling of bandwidth in each sideband to 16 GHz, two polarizations, and the new feature allowing two simultaneous receiver bands active (230 and 345 GHz). *wSMA* hinges on significant advances being made in wideband receiver design, and the availability of a dichroic plate to split the receiver bands. A back end to support the *wSMA* bandwidth without an increase in the number of analog IF channels—presently 32 across the eight antennas and two polarizations—is currently under development. The plan is to expand the instantaneously sampled contiguous usable bandwidth to 8 GHz per block. Referencing Table 1 we selected Adsantec ASNT7123A-KMA because of its elegant single core conversion, and economical cost. This part is also being developed for the ngEHT DBE.

Prior to the selection of the Adsantec 16 GSa/s part we experimented some years ago with single core 26 GSa/s 3-bit ADC then commercially available from Analog Devices Inc (ADI). Using this



Fig. 10. EHT digital VLBI backend as installed at the Institut de Radioastronomie Millimétrique (IRAM) PV 30 m telescope in Spain. Right-hand side upper rack are located the four R2DBE units. Two block downconverters are installed near the middle, and the VLBI backend computer is mounted on the bottom right. The rack on the left and the lower portion of the rack on the right hold the four Mark 6 recorders with four disk modules each, providing a total of about 1 PB in data storage.

device 3-bit 20 GSa/s conversion with data captured by the Xilinx Virtex 7 XC7VX690T Field Programmable Gate Array (FPGA) it has been demonstrated (Weintroub 2015) that this device is only 3-bits plus overflow is a little below requirements, and *sparkle code* artifacts were noticed in the output data.

Driven by the needs of industry, FPGAs optimized for digital signal processing, with as many as $\sim 12,000$ wide multipliers in a single chip, and ~ 30 Gbps asynchronous input-output on a single serial transceiver have become a powerful and flexible technology for astronomical DSP. The use of an industry-driven 100 Gbps wideband switch as the interconnect backbone has also been validated, and faster data rates are on the road map. These technologies, as well as tensor core GPUs for fast software driven programming are all in development for future wideband EHT and ngEHT systems.

Acknowledgements: This talk was given and abstract paper is submitted on behalf of the Event Horizon Telescope Collaboration <https://eventhorizontelescope.org/>. My travel to the IAR 60th Anniversary Conference (<https://congresos.unlp.edu.ar/iar60ws/>) was supported by the National Science Foundation under grant number AST-2034306. The Submillimeter Array is a joint project between the Smithsonian Astrophysical Observatory and the Academia Sinica Institute of Astronomy and Astrophysics. Development of the VLBI features of SWARM were funded by the Gordon and Betty Moore Foundation and National Science Foundation. We received generous donations of FPGA chips from the Xilinx University Program. Our research benefits from technology shared under open source license by CASPER (<https://casper.berkeley.edu>). This research has made use of NASA's Astrophysics Data System. We acknowledge the significance that Maunakea has for the indigenous Hawaiian people.

REFERENCES

- The Event Horizon Telescope Collaboration, et al. 2019a, *ApJ (Letters)*, 875, L1
- The Event Horizon Telescope Collaboration, et al. 2019b, *ApJ (Letters)*, 875, L2
- The Event Horizon Telescope Collaboration, et al. 2021, *ApJ (Letters)*, 910, L12
- The Event Horizon Telescope Collaboration, et al. 2022, *ApJ (Letters)*, 930, L12
- Hickish, J., et al. 2016, *Journal of Astronomical Instrumentation*, 5, 4
- Jiang, H., Liu, H., Guzzino, K., Kubo, D., Li, C.-T., Chang, R., Chen, M.-T. 2014, *PASP*, 126, 761-768
- Parsons, A., Backer, D., Siemion, A., Chen, H., Werthimer, D., Droz, P., et al. 2008, *PASP Vol. 120, Issue 873*, 1207
- Patel, N. A., Wilson, R. W., Primiani, R. A., Weintroub, J., Test, J., Young, K. H. 2014, *Journal of Astronomical Instrumentation*, 3, 1
- Primiani, R. A., et al. 2016, *Journal of Astronomical Instrumentation*, 5, 4
- Vertatschitsch, L., Primiani, R. A., Young, A., et al. 2015, *PASP*, Vol. 127, 1226
- Weintroub, J., et al., 2015, 26th International Symposium on Space Terahertz Technology, Cambridge, MA, 16-18 March, 2015
- Young, A., et al., *Proceedings of the IEEE International Symposium on Phased Array Systems & Technology*, Waltham, MA, October 18-21, 2016